



**HAL**  
open science

# Geology of the southern Monviso metaophiolite complex (W-Alps, Italy)

Michele Locatelli, Laura Federico, Philippe Agard, Anne Verlaguet

## ► To cite this version:

Michele Locatelli, Laura Federico, Philippe Agard, Anne Verlaguet. Geology of the southern Monviso metaophiolite complex (W-Alps, Italy). *Journal of Maps*, In press, 10.1080/17445647.2019.1592030 . hal-02108199

**HAL Id: hal-02108199**

**<https://hal.sorbonne-universite.fr/hal-02108199>**

Submitted on 24 Apr 2019

**HAL** is a multi-disciplinary open access archive for the deposit and dissemination of scientific research documents, whether they are published or not. The documents may come from teaching and research institutions in France or abroad, or from public or private research centers.

L'archive ouverte pluridisciplinaire **HAL**, est destinée au dépôt et à la diffusion de documents scientifiques de niveau recherche, publiés ou non, émanant des établissements d'enseignement et de recherche français ou étrangers, des laboratoires publics ou privés.



## Geology of the southern Monviso metaophiolite complex (W-Alps, Italy)

Michele Locatelli, Laura Federico, Philippe Agard & Anne Verlaquet

To cite this article: Michele Locatelli, Laura Federico, Philippe Agard & Anne Verlaquet (2019): Geology of the southern Monviso metaophiolite complex (W-Alps, Italy), Journal of Maps, DOI: [10.1080/17445647.2019.1592030](https://doi.org/10.1080/17445647.2019.1592030)

To link to this article: <https://doi.org/10.1080/17445647.2019.1592030>



© 2019 The Author(s). Published by Informa UK Limited, trading as Taylor & Francis Group



[View supplementary material](#)



Published online: 24 Mar 2019.



[Submit your article to this journal](#)



Article views: 131



[View Crossmark data](#)



## Geology of the southern Monviso metaophiolite complex (W-Alps, Italy)

Michele Locatelli <sup>a</sup>, Laura Federico<sup>b</sup>, Philippe Agard<sup>a</sup> and Anne Verlaquet<sup>a</sup>

<sup>a</sup>Institut des Sciences de la Terre de Paris (ISTeP), Sorbonne Université, Paris, France; <sup>b</sup>Dipartimento di Scienze della Terra, dell'Ambiente e della Vita (DISTAV), Università di Genova, Genova, Italy

### ABSTRACT

The Monviso metaophiolite complex (W. Alps) is an almost intact fragment of Tethyan oceanic lithosphere metamorphosed to eclogite-facies peak metamorphic conditions during Alpine subduction. This 1:20.000 scale geological map encompasses, in an area of ~35 km<sup>2</sup>, the Monviso Unit (MU) and the Lago Superiore Unit (LSU). Major focus was given to the Lower Shear Zone sub-unit (LSZ), where in the strongly deformed serpentinite-rich matrix are embedded blocks of variably brecciated metagabbros. Here, the occurrence of eclogite-facies mylonitic foliation (paragenesis: omphacite + rutile + garnet ± ex-lawsonite ± quartz) cut by breccia planes (cemented by omphacite + garnet ± ex-lawsonite) indicates brecciation at pristine eclogitic conditions. This map (i) provides new lithological, structural and morphological insights regarding the stratigraphy of the Monviso metaophiolite complex and (ii) supplies an unprecedented detail on the distribution of eclogite-facies breccia blocks inside the Lower Shear Zone that crosscuts the Lago Superiore Unit.

### ARTICLE HISTORY

Received 18 June 2018  
Revised 4 March 2019  
Accepted 5 March 2019

### KEYWORDS

Monviso Massif; Western Alps; shear zone; eclogitic breccia

## 1. Introduction

The presented 1:20.000 scale geological map (Main Map) covers an area of ~35 km<sup>2</sup> in the Monviso meta-ophiolite complex (Western Alps, Italy) which belongs to the Liguro-Piemontese units.

The Western Alps (Figure 1(a) and (b)) result from the convergence and subsequent collision between Adria and Europe plates, with the Liguro-Piemontese oceanic domain interposed, undergoing subduction (Coward & Dietrich, 1989; Laubscher, 1991; Ricou & Siddans, 1986; Schmid & Kissling, 2000).

In detail, the Liguro-Piemontese domain is formed by exhumed eclogite-facies tectonic slices, such as the Monviso meta-ophiolite, juxtaposed against lower grade sedimentary-derived terrains of the fossil accretionary wedge, such as the Schistes Lustrés (e.g. Agard et al., 2009, 2002; Marthaler & Stampfli, 1989; Plunder, Agard, Chopin, & Okay, 2013; Figure 1(a) and (b)).

In the Monviso area, the nappe stack shows, from West to East: (i) the Schistes Lustrés, (ii), the Monviso metaophiolite and the (iii) Dora Maira massif (Figure 1 (b)).

In recent years, a series of metagabbro blocks with peculiar clast-in-matrix structures were identified within the shear zones crosscutting the Monviso metaophiolite. Some of them are breccias composed of 1 to 10 cm-long fragments of eclogite mylonite cemented by interstitial eclogite-facies matrix. They have been interpreted either as produced by a brittle

event at eclogite-facies conditions (Angiboust, Langdon, Agard, Waters, & Chopin, 2012), potentially linked to intermediate-depth seismic events (Angiboust, Agard, Yamato, & Raimbourg, 2012) or as inherited pre-Alpine detachment fault rocks or sedimentary-derived breccias (Balestro, Festa, & Tartarotti, 2015; Festa, Balestro, Dilek, & Tartarotti, 2015).

The aims of this work are therefore: (i) to provide an update of the geological map of the area; (ii) to map the occurrence and distribution of brecciated eclogite-facies bodies inside the Monviso metaophiolite complex, and (iii) to describe the structures, internal organization and composition of the breccias. Additionally, a possible interpretation of their origin is proposed.

## 2. Methods

The Main Map results from original fieldwork at 1:10.000 scale using the topographic base of the Carta Tecnica Regionale (CTR maps) of the Regione Piemonte -Italy- (<http://www.geoportale.piemonte.it/cms/>).

The precise location of metagabbro blocks was obtained by GPS positioning (latitude, longitude and altitude); the distribution analysis was performed on those with preserved primary contacts with the shear zone matrix. The volume of each block, assumed to be ellipsoidal, was estimated by direct, in-loco measurement of height, width and length crosschecked with aerial-image measurements (of width and length only) run with google Earth Pro™.

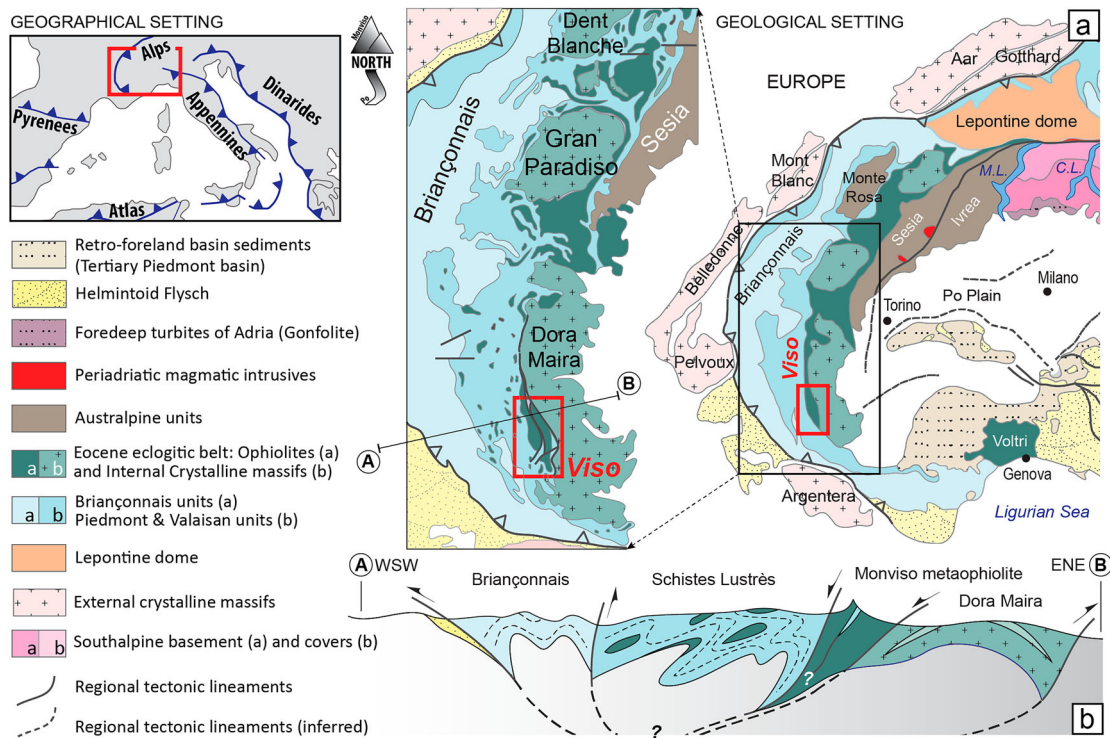


**Figure 1.** (a) Tectonic sketch of the Western Alps. The Eocene eclogitic belt (deep-green) is exposed on the upper-plate side of the orogen, between the Frontal wedge (light blue) and the remnants of a Late Cretaceous doubly-vergent wedge (yellow). In the inset, a detail of the eclogite belt and the frontal wedge with the localization of the Monviso metaophiolite. (b) Simplified geological cross section (A–B) that depicts the major structures and tectonic units across the Alpine edifice; color-code as in the geological map. Maps are modified after Malusà, Faccenna, Garzanti, and Polino (2011) and Agard, Yamato, Jolivet, and Burov (2009). The geological cross-section is derived from Guillot, Schwartz, Hattori, Auzende, and Lardeaux (2004).

Field data were digitalized (Coordinate System WGS 1984, UTM Zone 32N) and projected on a digital topographic base derived by the DTM of Regione Piemonte. The new lithological, structural and geomorphological data were compared and locally integrated with those from Balestro, Fioraso, and Lombardo (2013) and Lombardo (1978).

The quaternary geology results from original mapping and was later implemented by aerial image analysis.

### 3. Geological setting

The Monviso metaophiolite complex represents a well-preserved fragment of Tethyan oceanic lithosphere (Figure 2(a–c)). It used to be subdivided into six tectonometamorphic units (Lombardo, 1978) interpreted, from both petrological and structural evidences, as a deep subduction mélangé where tectonic slices were detached from different depths and later exhumed in a weak, serpentized subduction channel (e.g. Guillot et al., 2004; Schwartz et al., 2000).

This interpretation was challenged by Angiboust, Agard, Raimbourg, Yamato, and Huet (2011, 2012) who suggested (based on new petrographic evidences and P–T estimates) that the Monviso metaophiolite was rather formed by two main coherent tectonometamorphic units, the first one being overturned on

the second one: the Monviso s.s. unit (MU), with peak P–T conditions at ca. 480°C/22 kbar, and the Lago Superiore Unit (LSU) (Figure 2(a–c)).

Nevertheless, this interpretation did not reach general consensus: from the study of block-in-matrix structures preserved at the top of Dora Maira Massif and inside the LSZ (Baracun shear zone *Auct.*), Balestro et al. (2018; Balestro, Festa, & Tartarotti, 2015; Balestro, Fioraso, & Lombardo, 2013; Balestro et al., 2014) and Festa et al. (2015) proposed the occurrence in the Monviso metaophiolite complex of a reworked Oceanic Core Complex. Thus, the internal structure of the metaophiolite was again revisited as a series of units juxtaposed across major shear zones not developed at high-pressure but resulting from the reactivation of pre-alpine structures (e.g. oceanic detachment and/or slab-inherited bending faults), rehabilitating the interpretation of Monviso metaophiolite as a tectonic-mélangé s.s. (Festa, Pini, Dilek, & Codegone, 2010).

Our contribution focuses mainly on the LSU (Figure 2(a)), which comprises, from bottom to top: serpentized lherzolite intruded and/or capped by late Jurassic Mg–Al and/or Fe–Ti gabbros; banded tholeiitic basalts; microgabbros and mixed calcareous/pelitic Cretaceous metasediments (Balestro, Festa, et al., 2015; Balestro, Fioraso, et al., 2013; Balestro, Lombardo, et al. 2014; Castelli, Rostagno, & Lombardo, 2002; Lombardo,

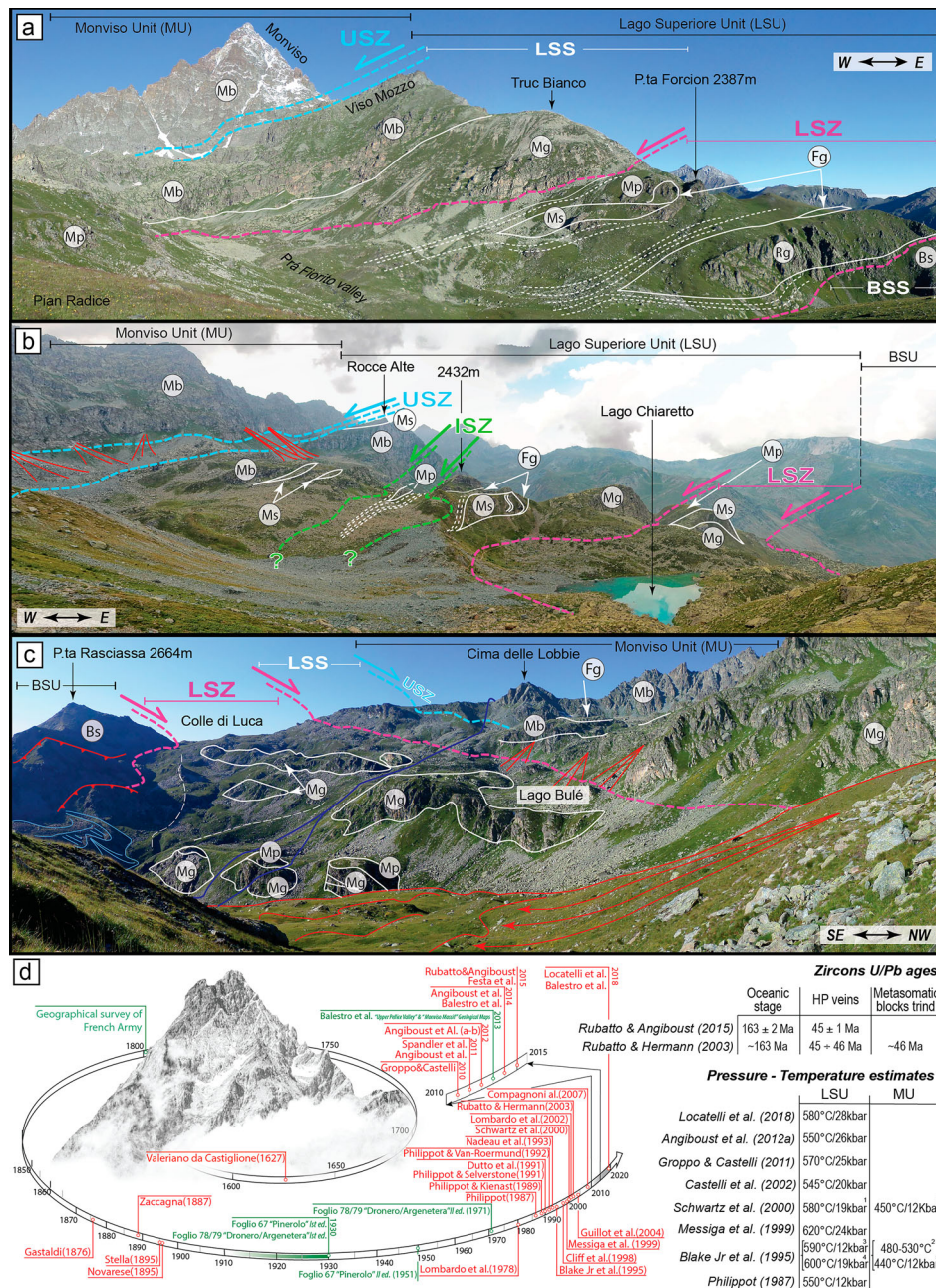


**Figure 2.** (a) Panoramic view from Pian Radice toward NW depicting the inner organization of the Lago Superiore Unit (LSU). Retrogressed Mg-Al metagabbro slices are continuously enveloped in the Lower Shear Zone (LSZ) from P.ta Forcion to Colle di Luca, together with peridotite slivers and minor bodies of Fe-Ti metagabbros and breccia blocks. Metabasites and metabasalts are always underlined by Mg-Al metagabbros up-to 300 meters thick. At the top of the LSU, the Upper Shear Zone (USZ) marks the boundary with the Monviso Unit (MU). The latter is constituted by a thick (up-to 500 meters), overturned sequence of metabasites with minor metagabbros capped by a thin (max 15 meters thick) metasediments cover (the latter largely outcropping W of Lago Grande di Viso). BSS = Basal Serpentine sub-unit. LSS = Lago Superiore s.s sub-unit (b) Panoramic view from the base of the Viso Mozzo toward the north, with highlighted the limits of the Lower, Intermediate and Upper shear zones. On the left of the figure, partly covered by recent rock-fall deposits, the terminal moraine developed during the maximum advance of the NE Monviso 'Pyrenean-Type' glacier in the Little Ice Age (LIA). Note that the 'heart' shape of Chiaretto lake is derived by the accumulation of rock-fall debris produced by the collapse of the Coolidge glacier in 1989 (Mortara & Dutto, 1990) (c) Panoramic view to the south of the Bulé valley taken from the base of the eastern flank of the Peiro Jauno flank, with enlightened the slivers of Mg-Al metagabbros and metaperidotites scattered in the LSZ matrix. The blue, continuous lines highlight the faults system that crosscuts the Bulé valley resulting in the apparent dextral displacement of pre-existing structures. On the left of the figure we highlighted the trenches produced by the deep seated gravitational slope deformations (DSGSD) occurring at the western flank of Costa Pelata (N of P.ta Rasciassa). The volume of the DSGSD is able to deviate the underlying rock-glacier at its base (now inactive). (d) Timeline summarizing the main geological works relative to the Monviso area. The study of Valeriano di Castiglione (Abbot from Milan) was the first to evaluate the elevation of Monviso: 1664 meters above the Chiaretto Lake (~3925 meters above the sea level, an amazing result considering that the elevation of the 'Re di Pietra' is 3841 meters a.s.l.). In the table, a summary of PT investigation and ages for the Monviso metaophiolite complex: average PT estimate from Schwartz, Lardeaux, Guillot, and Tricart (2000) are from (1) Lago Superiore area and (2) Passo Gallarino area. The Average PT estimate from Blake, Moore, and Jayko (1995) are from (2) Passo Gallarino area, (3) Lago Superiore Sub-Unit and (4) Lower Shear Zone Sub-unit, (5) Monviso Unit.

1978). Strong lateral variations in lithostratigraphy, with one or more of the above horizons missing, were attributed to an irregular seafloor structure typical of slow spreading oceans (e.g. Lagabriele & Lemoine, 1997). Nevertheless, only slightly different eclogitic P-T peaks (Figure 2(d)) were calculated by different authors for the LSU: 590–600°C/12–19 kbar (Blake et al., 1995), 620°C/24 kbar (Messiga, Kienast, Rebay, Riccardi, & Tribuzio, 1999), 580°C/19 kbar (Schwartz et al., 2000), 545°C/20 kbar (Castelli et al., 2002), 570°C/25 kbar (Groppo & Castelli, 2010) and 550°C/26 kbar (Angiboust, Langdon, et al., 2012), 580°C/28 kbar (Locatelli, Verlaquet, Agard, Federico, & Angiboust, 2018).

The original stratigraphic sequence is partly disrupted by shear zones (Angiboust et al., 2011, 2012; Festa et al., 2015; Lombardo, 1978; Philippot & Kienast, 1989): the Upper, Intermediate and Lower Shear Zones (USZ, ISZ and LSZ respectively; Figure 2(a–c)). Since P-T conditions are undistinguishable on either side of the shear zones (Angiboust, Langdon, et al., 2012), vertical displacements along them are probably less than km-scale. In this contribution we particularly focus on the LSZ.

#### 4. Geology of the mapped area (Tectonostratigraphy)

The Main Map encompasses the LSU and the MU. The two units show a similar tectono-metamorphic history and recorded four main tectono-metamorphic events:

- (I) The Pre-Alpine, oceanic-stage event, responsible for the primary lithostratigraphy of the ophiolite, followed by three successive Alpine stages, describing:
  - (II) the peak-metamorphism eclogitic event (D1), leading to the formation of S1.
  - (III) the exhumation-stage Blueschist event, characterized by the regional development of the S2 foliation.
- (IV) the continental-collision event, recorded by D3 greenschist-facies structures.

More details on tectono-metamorphic events and related structures are presented in *par. 5*.

Additionally, applying the definition of tectonostratigraphic units after De La Pierre, Lozar, and Polino (1997), we define sub-units of the LSU the Basal Serpentinite sub-unit (BSS), the Lower Shear Zone sub-unit (LSZ) and the Lago Superiore *s.s* sub-unit (LSS), including the Intermediate and Upper Shear Zones – ISZ and USZ. Figure 2(a–c). A list of all abbreviations used in this paper to describe the different tectonostratigraphic units is listed in the Appendix.

#### 4.1. The Lago Superiore Tectonostratigraphic Unit (LSU)

##### 4.1.1. The Basal Serpentinite sub-unit (BSS)

The basal serpentinite sub-unit crops out continuously in the studied area from Colle della Gianna (where it is up to 1000 m-thick) to the Punta Rasciassa area (where its thickness decreases to 500 meters) and corresponds to the lowest sub-unit of the Monviso Metaophiolite complex. It is composed of antigorite serpentinites -Bs- with pervasive, magnetite-rich foliation (Figure 3(a)). The peridotite pre-alpine mineral assemblage is preserved as relics of pyroxenes only in the poorly deformed areas. Meter-sized rodingitic-metagabbro dykes -Rd- are locally aligned along the foliation (Figure 3(b)).

M- to hm-size boudins composed of Mg-Al and Fe-Ti metagabbros (*Mg* and *Fg*, respectively) are discontinuously scattered in the BSS (e.g. Figure 3(c)). The mylonitic Mg-Al metagabbros are mainly composed of omphacite, clinozoisite, Cr-rich amphibole (*smaragdite Auct.*) with minor albite and actinolite in more retrogressed portions; eclogite-facies boudins (e.g. with Fe-Ti metagabbro composition) are scattered in the foliation and are crosscut by high-pressure-veins (paragenesis: garnet + omphacite; Figure 3(d)).

The eclogite-facies Fe-Ti metagabbros crop out as dm-sized boudins east of Costiera dell'Alpetto Cliff and south of Pian del Re. Their textures vary progressively from cm-sized cores composed of deep-green clinopyroxene and garnet to dm-thick mylonitic bands composed of omphacite, garnet, abundant rutile and rare Na-amphibole-rich bands. M-sized blocks with the same fabrics and mineralogy crop out at the base of the LSZ (see *par. 6* for more details).

##### 4.1.2. The Lower Shear Zone sub-unit (LSZ)

The Lower Shear Zone sub-unit marks the boundary between the Basal Serpentinite sub-unit and the Lago Superiore sub-unit. In the map it extends 15 km along strike, from the south (Colle di Luca pass) to the north (Rocce Fons). Its thickness varies along strike, from a minimum of ~250 m in the Punta Forcione area and a maximum of ~600 m in the Pian Radice area.

Its internal structure corresponds to a tectonic mélange (*sensu Festa et al., 2010*), where a pervasively foliated antigorite schists matrix encloses meter-sized blocks and decametre-sized slivers (Figure 3(e)) composed of (i) eclogite-facies breccia *s.s* -Eb- (also composing the bulk of Type1 blocks), (ii) retrogressed Mg-Al metagabbro -Rg- crosscut by eclogite-facies breccia layers (e.g. in Type2 blocks), (iii) unbrecciated, eclogitic Fe-Ti metagabbro -Fg- (e.g. Type 3 blocks), (iv) metaperidotite -Mp-, (v) metasediments *s.s.* -Ms-, (vi) rodingitic metagabbro dykes -Rd- (Figure 3(f))

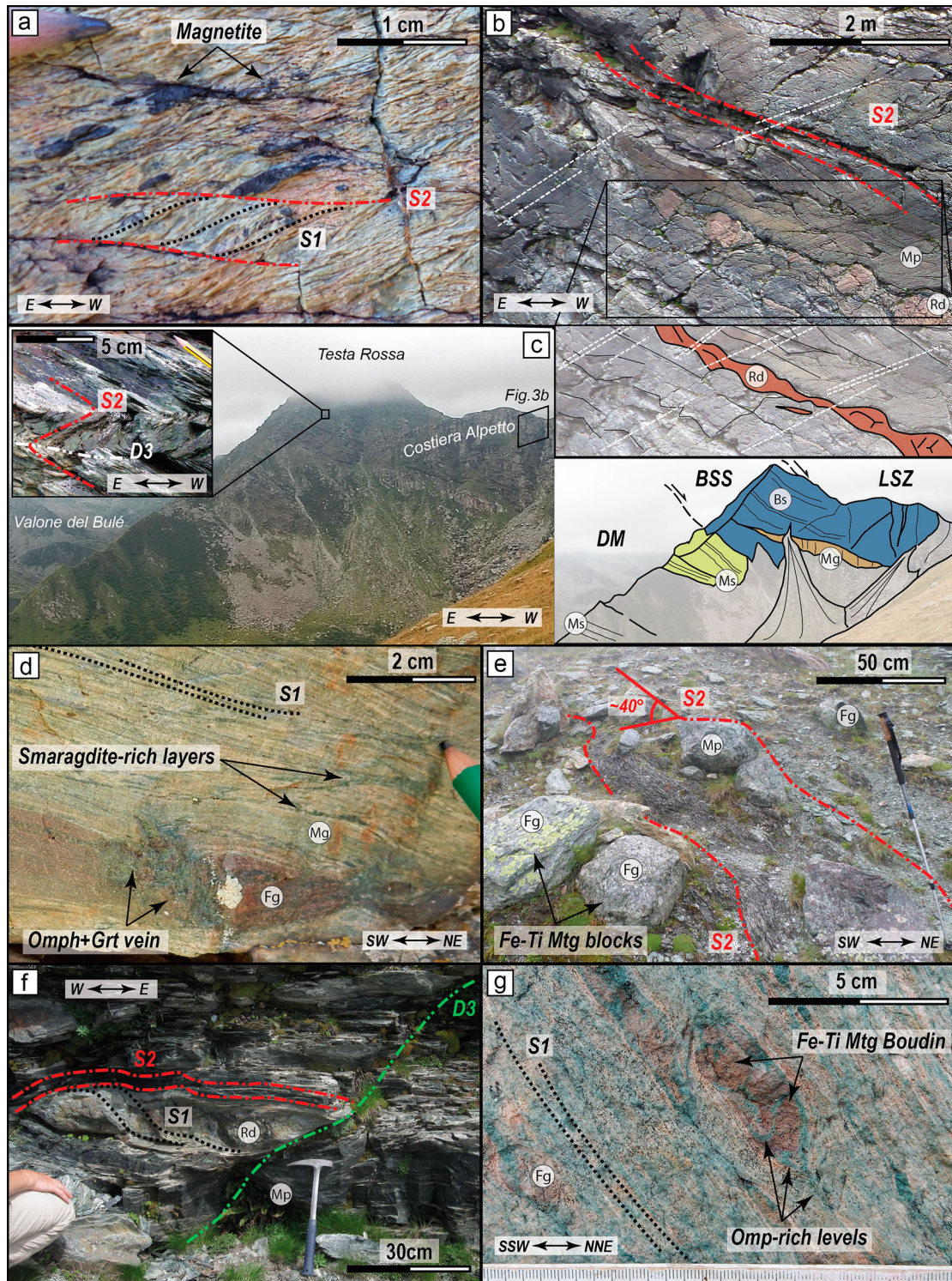


**Figure 3.** (a) Close-up view of the metaperidotite composing the bulk of the BSU. In evidence the SC-structure with S1 foliation (underlined by magnetite-beds) transposed by the S2 foliation. (b) Boudinated rodingitic dyke (white arrows) enclosed in the meta-peridotites, east of Alpetto lake. In evidence the W-dipping S2 foliation and the glacial striations carved on the glacier-polished basal serpentinites (white full lines). (c) Panoramic view of the basal serpentinite cliff E of Alpetto lake. The cartoon highlights the metagabbro mega-boudin (note its lighter colour in the photo) and the metasediments pinched in-between the Monviso metaophiolite (W) and the Dora Maira massif. In the inset, a detail of the parasitic W-verging folds developed in the serpentinite during the D3 deformation stage. (d) Centimetre-sized boudin composed Fe-Ti metagabbro -Fg- enclosed in a Mg-Al metagabbro -Mg- sliver. In evidence, at the contact between the two gabbros, a newly-formed crystallization composed by omphacite + garnet ('vein'), comparable to the matrices observed in eclogite-facies breccias (more details in §6). (e) Typical appearance of the antigorite-rich serpentinite constituting the bulk of the LSZ and ISZ. The finely-crenulated serpentinites envelope numerous blocks of variable size composed of Mg-Al and Fe-Ti metagabbros (Mg and Fg, respectively), massive metaperidotite (Mp) and, locally, metasediment slivers. The blocks distribution is only apparently chaotic, as shown in Figure 7(c). (f) Rodingitic dyke (Rd) embedded in a foliated serpentinite sliver from the LSZ. The pervasive foliation developed in the metaperidotite (Mp) is coeval to the stage D2. D3 deformation leads to the development of disjunctive surfaces crosscutting at high-angle the S2. Photo taken W of Rocce Sbiasere. (g) Close-up view of Fe-Ti metagabbro composed of garnet + rutile + omphacite. Boudins composed by Grt + Rtl (block SW of P.ta Forcion) are often found aligned along the S1 foliation of the metagabbro.

and (vi) rare jadeitite (more details on the eclogitic metagabbro blocks in *par. 6*).

#### 4.1.3. The Lago Superiore S.S. sub-unit (LSS)

The LSS is composed of metabasites, Mg-Al metagabbros and metasediments, with minor Fe-Ti metagabbros. It is bounded at the top by the USZ, defined by the occurrence of chlorite- and talc-bearing antigorite schists.

The eclogitic Fe-Ti metagabbros -Fg- (Figure 3(g)) consist in decametre- to meter-sized masses found at the top both of Mg-Al metagabbros -Mg- and metabasites -Mb-. Their texture varies from dm-sized, coarse low-strain domains composed of clinopyroxene + garnet  $\pm$  lawsonite-pseudomorphs to progressively more deformed, m-thick mylonitic bands composed of omphacite, garnet and rare ex-lawsonite-rich bands with abundant rutile aligned along the pervasive foliation (e.g. Figure 3(g)). The mylonitic foliation was acquired during prograde, eclogite-facies deformation (e.g. Philippot & van Roermund, 1992; Locatelli et al., 2018).

Locally, especially in the Lago Superiore area, eclogite-facies breccia blocks -Eb- crop out in the ISZ. Moreover, m-scale metabasaltic blocks (hanging wall of the ISZ) are found in the ISZ together with scarce metasedimentary blocks and massive serpentinite blocks (e.g. Figure 3(e)).

The Mg-Al metagabbros (Figure 4(a–d)) correspond to the smaragdite-bearing metagabbros of the literature (e.g. Lombardo, 1978). They crop out at the base of the metabasites between the NE flank of the Viso Mozzo to the Colle di Luca. These medium-to-fine grained mylonitic metagabbros show alternate clinozoisite-rich and omphacite-rich bands (Figure 4(a) and (b)) with subordinate glaucophane (Figure 4(c)). Garnet is present only near Fe-Ti metagabbro boudins (e.g. Figure 4(a)). The greenschist retrogression leads to localized crystallization of albite, epidote and tremolite/actinolite (e.g. at the contact with the LSZ antigorite-rich matrix or on late-stage fault planes; Figure 4(d)). Layered to massive metatroctolites -Mt- crop out as meter-thick boudins in the cliff W of Lago Fiorenza, intercalated to finely crenulated, decimetre- to meter-thick metaperidotites -Mp-.

The foliated metabasites show a banded texture (Figure 4(e) and (f)) consisting of alternate albite-, epidote-rich and Na-amphibole/actinolite-rich levels. Boudins of eclogitic metabasites (composed by omphacite + clinozoisite; Figure 4(e)) locally occur along the pervasive, glaucophane-rich foliation. Dm-scale, pillowed textures are locally preserved.

The metasediments -Ms- (Figure 4(g) and (h)) crop out mainly at the top of the LSS as decametre- to meter-thick slivers stratigraphically above the metabasites (e.g. Figure 2(b)). Minor m-thick bodies crop out discontinuously E of Passo Gallarino between the

metabasites and the Fe-Ti metagabbros. They mainly consist of mylonitic calcschists with minor micaceous-rich levels, micaceous marbles and quartz/phengite-rich garnet-bearing micaschists (Figure 4(g)) intercalated with polymictic metabreccias and meta-sandstones (Figure 4(g) and (h)).

#### 4.2. The Monviso Tectonostratigraphic Unit (MU)

The MU reaches a maximum thickness of  $\sim$ 900-m across the E flank of Monviso and is bounded to the W by the overlying Queyras Schistes Lustres. It is an overturned sequence of metagabbros and metabasalts, with minor metasediments discontinuously cropping out W of Lago Grande di Viso and W of Passo Gallarino. The metabasalts -Fb- are aphyric and porphyritic, locally with brecciated and pillowed textures. They show a well-developed metamorphic layering with alternating epidote-rich and Na-amphibole and tremolite/actinolite-rich layers.

Here, the metasediments -Mus- consist of phengite- and garnet-bearing metacherts overlaying calcschist interbedded to quartz/phengite-rich garnet-bearing micaschists.

### 5. Structures

We recognized five main tectonometamorphic phases, classified as D0, D1, D2, D3 and D4 to be consistent with the literature (e.g. Balestro et al., 2013). The primary surfaces (i.e. the S0) correspond to the primary lithological contacts incorporated in the composite fabric of the Alpine tectono-metamorphic events (e.g. Figure 4(a)), though pristine magmatic foliation was never observed in the metagabbros or metabasalts.

The D1 phase (Figure 5(a) and (b)) is locally preserved in the metagabbros (Figures 3(d), (g) and 4(a–c)), in dm-sized boudins in metabasites (Figure 4(e)), in metaperidotite lenses from LSZ (Figure 3(a)) and rodingitic dykes (Figure 3(f)). It is coeval with peak eclogite-facies metamorphism (e.g. associated in Fe-Ti metagabbros to omphacite + almandine-rich garnet + rutile  $\pm$  glaucophane assemblage). Where preserved, the S1 foliation is mostly NW-SE striking and dips to S/SW at variable angles (Figure 5(a) and (b)).

The D2 stage (Figure 5(c–f)) is the most pervasive deformation event recorded in the Monviso metapliolite (e.g. Figures 3(a–d), (f) and 4(e–h)). It develops during blueschist-facies retrogression. The lithological contacts, as well as the synmetamorphic shear zones bounding the W- to SW-dipping units (e.g. LSZ; Figure 4(e)), are parallel to the S2 pervasive foliation. The latter is generally N/NW-S/SE striking with shallow-to-moderate SW-dip (e.g. Figure 5(c–f)) and corresponds to the axial plane of tight to isoclinal D2 folds.

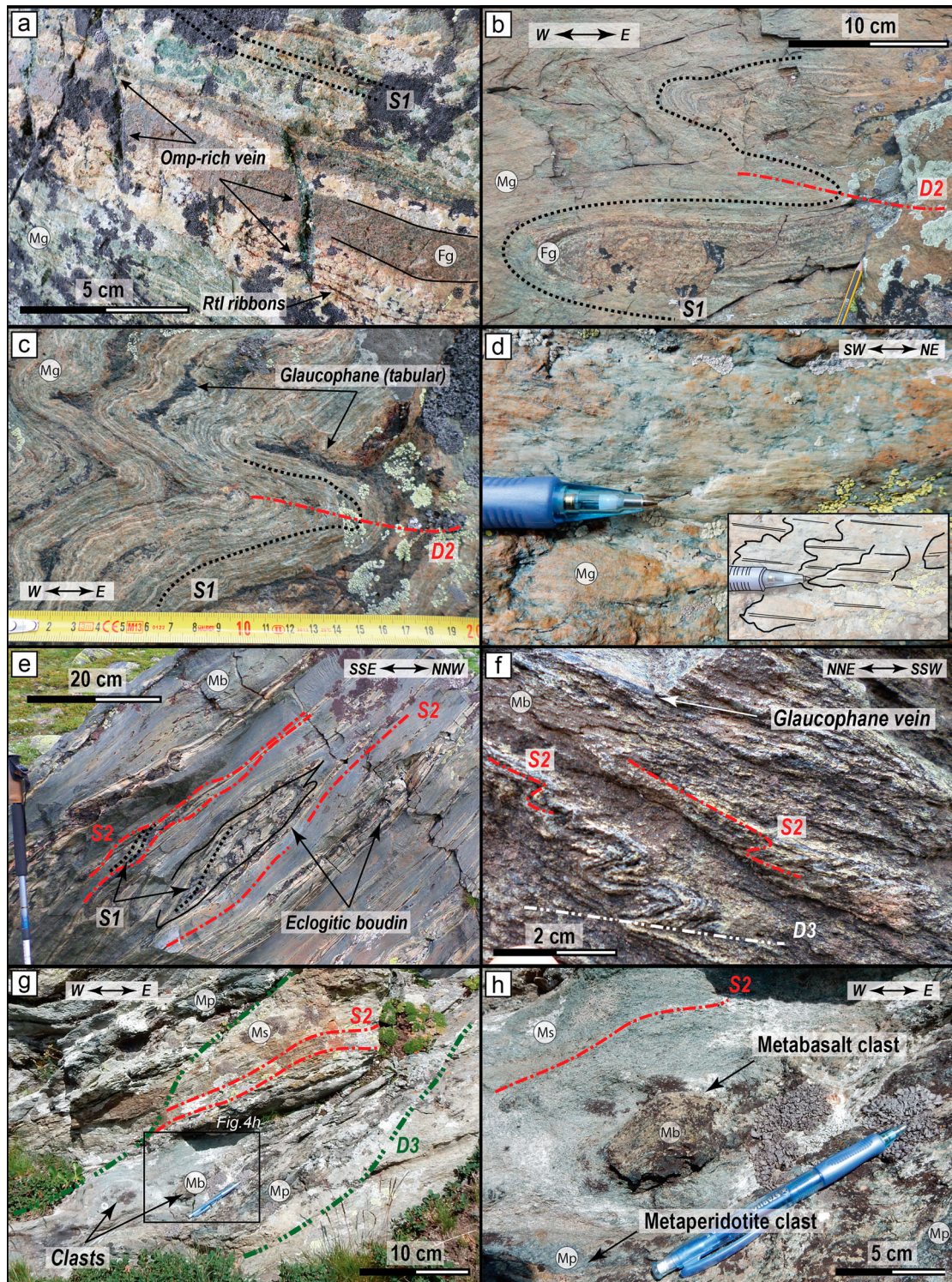


**Figure 4.** (a) Highly-deformed Fe-Ti metagabbro boudin (Grt + Rtl ± Omp, Fg) embedded in the S1 schistosity of a Mg-Al metagabbro (Omp + Ep ± Rtl) block. In evidence the Omp-rich veins, developed sub-perpendicularly to the Mg-Al Mtg foliation, crosscutting the boudin and disappearing in the first centimetres of the Mg-Al metagabbro. The latter in the portions around the boudins (evidenced in the figure by solid lines) have a composition enriched in Ep (brownish ribbons subparallel to S1) and Grt. Block B70, NE of Rocce Sbiasere. (b) Example of recumbent syn-D2 folds recorded in the retrogressed Mg-Al metagabbro slivers dispersed in the LSZ (photo from Ghincia Pastour area). (c) Close-up view of a retrogressed Mg-Al metagabbro with static crystallization of glaucophane at the hinge of syn-D2 folds (Rg east of Alpetto lake, block B7). (d) Slickenlines on a fault plane (181/78) cutting mylonitic Mg-Al metagabbros. The fault has striae developed on albite and epidote. Their shearing direction and the orientation of steps on fault plane indicate dextral transtensive kinematic. Picture taken in the Bulé valley, south of Colle di Luca pass. (e) Eclogitic boudins (with preserved S1: paragenesis Omp + Ep) embedded in the S2 foliation of metabasites outcropping SSE of the Gallarino lake. (f) Close-up view of the recumbent folds W-verging, syn-D3, developed in the finely foliated metabasites outcropping at the base of the NE flank of Viso Mozzo. (g, h) Metasediments (Ms) outcropping structurally above the metabasites of the Lago Superiore Sub-unit. Meter-scale 'SC' structures related to D3 deformation phase displace the S2 foliation; cm-to-dm-scale clasts composed by metabasites (Mb) and metaperidotite (Mp) and metagabbros (here not in the picture) are enveloped in finely-grained quartz- and mica-bearing calcchists along S2. Photo taken SE of Lago Grande di Viso.

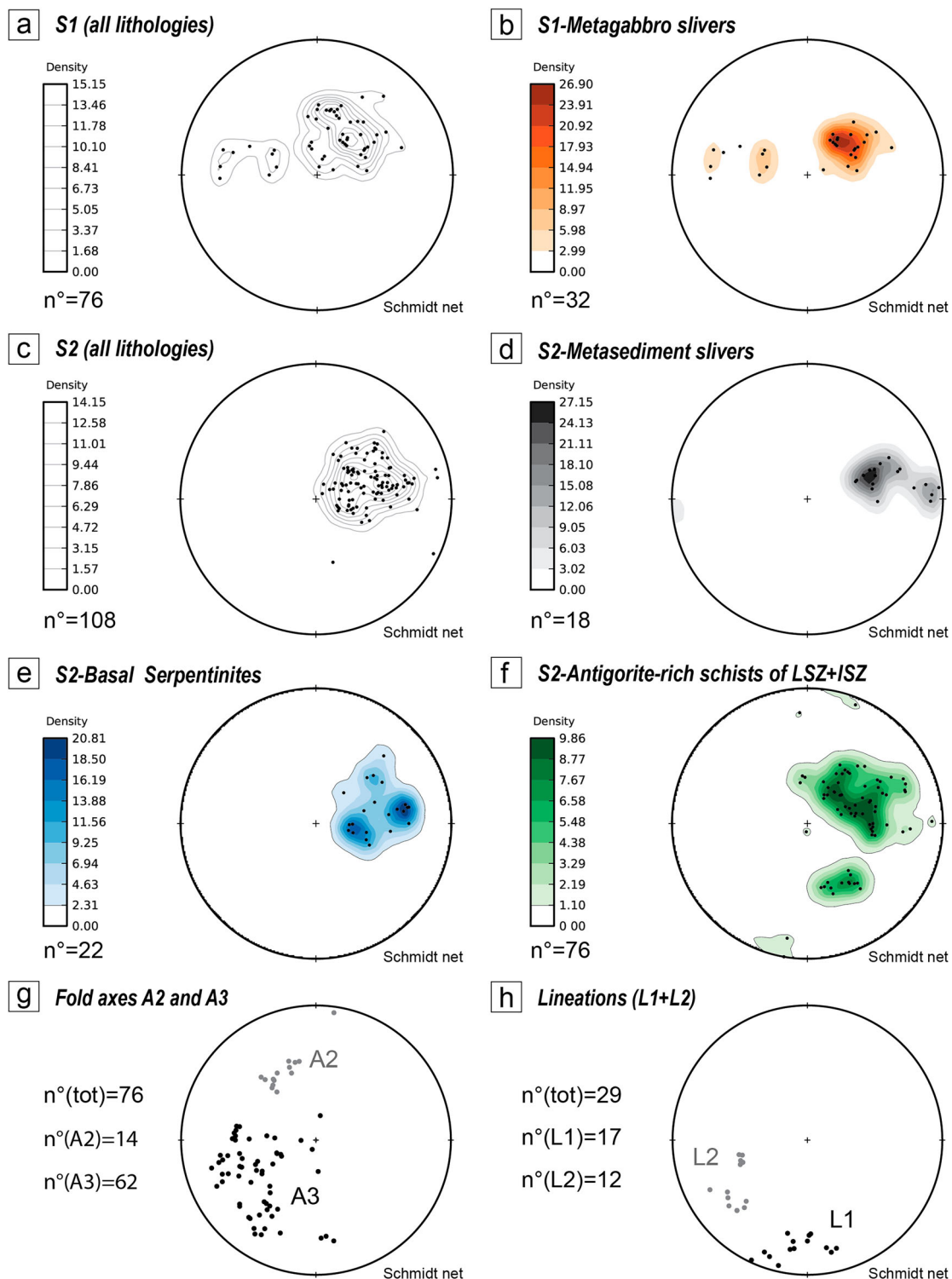


**Figure 5.** Foliation S1 sorted by lithology: (a) all lithologies; (b) Mg-Al metagabbros slivers disseminated in the LSZ; foliation S2 sorted by lithology: (c) all lithologies; (d) metasedimentary slivers disseminated in the LSZ and ISZ; (e) massive antigorite-rich serpentinites of the BSU; (f) antigorite-rich serpentinite of LSZ and ISZ. The clustering of S1 poles is linked to the isoclinal folding observed in the retrogressed Mg-Al metagabbros slivers dispersed in the LSZ. In general, S1 foliations show a common dip-direction towards SSW. The S2 poles, representing the regional foliations, describe a well clustered dip-direction towards SW. (g-h) Fold axis and lineations poles -all lithologies-. Fold axes were observed for the D2 and D3 folding. Lineations were observed only on pristine D1 and D2 foliation planes. For D3, no clear lineations were recognized. All the stereogram are plotted on Schmidt net, lower hemisphere.

The L2 stretching-lineation (Figure 5(h)) has constant NE-SW trend and SW-WSW dip. Macroscopically, in the metabasites and the metagabbros from the LSU, the S2 is defined by mm-thick beds of

glaucofane ± clinozoisite alternated to levels richer in clinozoisite ± chlorite ± smaragdite (e.g. Figure 4(e) and (f)). South-east of Passo Gallarino, the D2 phase brings about boudinage of eclogite-facies metabasites

and development of S–C structures (e.g. Figure 4(e)). At the opposite, in the retrogressed Mg–Al metagabbro scattered along the LSZ sub-unit, no dynamic recrystallization under blueschist/greenschist facies is observed. It is rather recorded, along the foliation and in the hinge of the recumbent folds, the static recrystallization of glaucophane ± epidote and actinolite (e.g. Figure 4(c)). Within the antigorite-schist matrix of the shear zones the S2 results in cm- to dm-long disjunctive shear surfaces whereas no univocal evidences of L2 lineation was observed.

The D3 stage is characterized by open to close folds (e.g. Figures 3(c) and 4(f)). In the metabasites and metagabbros from the LSU, the D3 results in W-SW-verging parasitic-folds and local development of SC-structures where the S2 is dragged on newly-formed epidote-, actinolite- and chlorite-bearing S3 schistosity (Figure 4(f)).

In the antigorite-rich schists of the shear zones the D3 defines a finely banded crenulation with W-WSW verging folds in less deformed areas (Figure 3(c)); increasing deformation results in disharmonic folding with rootless geometries progressively flattening into W-dipping shear bands. Development of high-angle spaced cleavage inside less competent rocks is also recorded (e.g. Figures 3(f) and 4(g)).

All the listed structures are finally crosscut by a network of high-angle transtensive faults, the D4 stage. A major NE/SW-striking fault system has been observed in the Bulè Valley, while another high-angle, W-dipping fault is emplaced E of Lago Grande di Viso. Both of these fault systems show dextral transtensive kinematics (Figure 4(d)).

## 6. The eclogitic metagabbro blocks

The positions of 195 eclogitic metagabbro blocks scattered in the three shear zones were precisely mapped; of these, 55 samples were drilled inside clasts, matrix, and at clast/matrix contacts for subsequent analysis (see Locatelli et al., 2018 for details).

### 6.1. Block types and distribution within shear zones

#### 6.1.1. Eclogitic metagabbros in the LSZ

**6.1.1.1. Block types.** The metagabbro blocks in the LSZ encompass both Fe–Ti and Mg–Al metagabbros (Locatelli et al., 2018).

Their morphology, structure and mineralogy allow to classify them into three groups:

(1) **Type1 blocks** (Figure 6(a)): composed of brecciated metagabbros only, are the most representative of the eclogitic bodies dispersed in the LSZ (62% of mapped blocks, Min Vol. 0.05 m<sup>3</sup>, Max Vol. 2613,81 m<sup>3</sup>). They present a peculiar clast-

in-matrix structure (Figure 6(a–c)), with clasts of mylonitic Fe–Ti metagabbros and rare Mg–Al gabbros (10% of modal amount), cemented by omphacite-rich matrix (±garnet and lawsonite) lacking any foliation (Figure 6(c–f)). Mylonitic fabric inside the clasts is marked by syn-kinematic garnet, omphacite and rutile (Figure 6(g) and (h)). Matrix proportions vary, from block to block, from less than 10 vol.% to up to more than 50 vol.%.

(2) **Type2 blocks** (22% of mapped blocks, Min Vol. 1.51 m<sup>3</sup>, Max Vol. 125663.71 m<sup>3</sup>): are mainly composed of Mg–Al metagabbros showing a medium-to-fine grained clinozoisite-rich and omphacite-rich mylonitic foliation (Figure 7(a)). Embedded boudins of Fe–Ti metagabbros (up to 5 m thick) are common. In Type2 blocks the mylonitic foliation is in places abruptly truncated by planes of brecciated Type1 Fe–Ti metagabbros (Figure 7(a)). Biggest bodies consist of five main lenticular sheets (up to 50-m thick; e.g. Colle Di Luca, Punta Murel and Lago dell’Alpetto; Figure 7(b)) generally NNE–SSW-striking north of Prá Fiorito Valley and NNW–SSE-striking in the Lago Bulè area. Here eclogite-facies breccia planes always bound the hm-scale Type 2 blocks on their western flank (i.e. facing the Mg–Al metagabbro cliff, dipping 20° to 60° to the W) and are absent on the other side.

(3) **Type3 blocks:** finely-foliated to massive, unbrecciated Fe–Ti metagabbros (16% of mapped blocks, Min Vol. 1.56 m<sup>3</sup>, Max Vol. 6.00 m<sup>3</sup>). Coarse grained fabrics are preserved in the core of the largest blocks (>10 m<sup>3</sup>; Figure 7(c)) and consist in almost undeformed coronitic garnet crystallizing around megacrysts of omphacite, which were interpreted as pseudomorphs after magmatic pyroxene and plagioclase (Groppo & Castelli, 2010; Locatelli et al., 2018; Lombardo, 1978; Pognante & Kienast, 1987). All blocks are coated by late, variably thick metasomatic rinds formed at the expense of the eclogite-facies matrix.

#### 6.1.1.2. Metagabbro block distribution within the LSZ.

Detailed mapping along the 11 km-long LSZ suggests a non-chaotic distribution of the metagabbro blocks: Type1 and Type2 blocks preferentially crop out in the intermediate-to-upper part of the shear zone, whereas unbrecciated Type3 blocks are restricted to the lower part of the LSZ (Figure 7(d)).

Block distribution in the shear zone also depends on the volume of the blocks: the largest Type1 breccia blocks (80% of mapped Type1 blocks, average volume >50 m<sup>3</sup>) are restricted to the upper part of the shear zone, whereas smaller blocks (20%, with average volume of 10 m<sup>3</sup>) are spread in the lower half of the shear zone (e.g. below the biggest Type2 blocks).

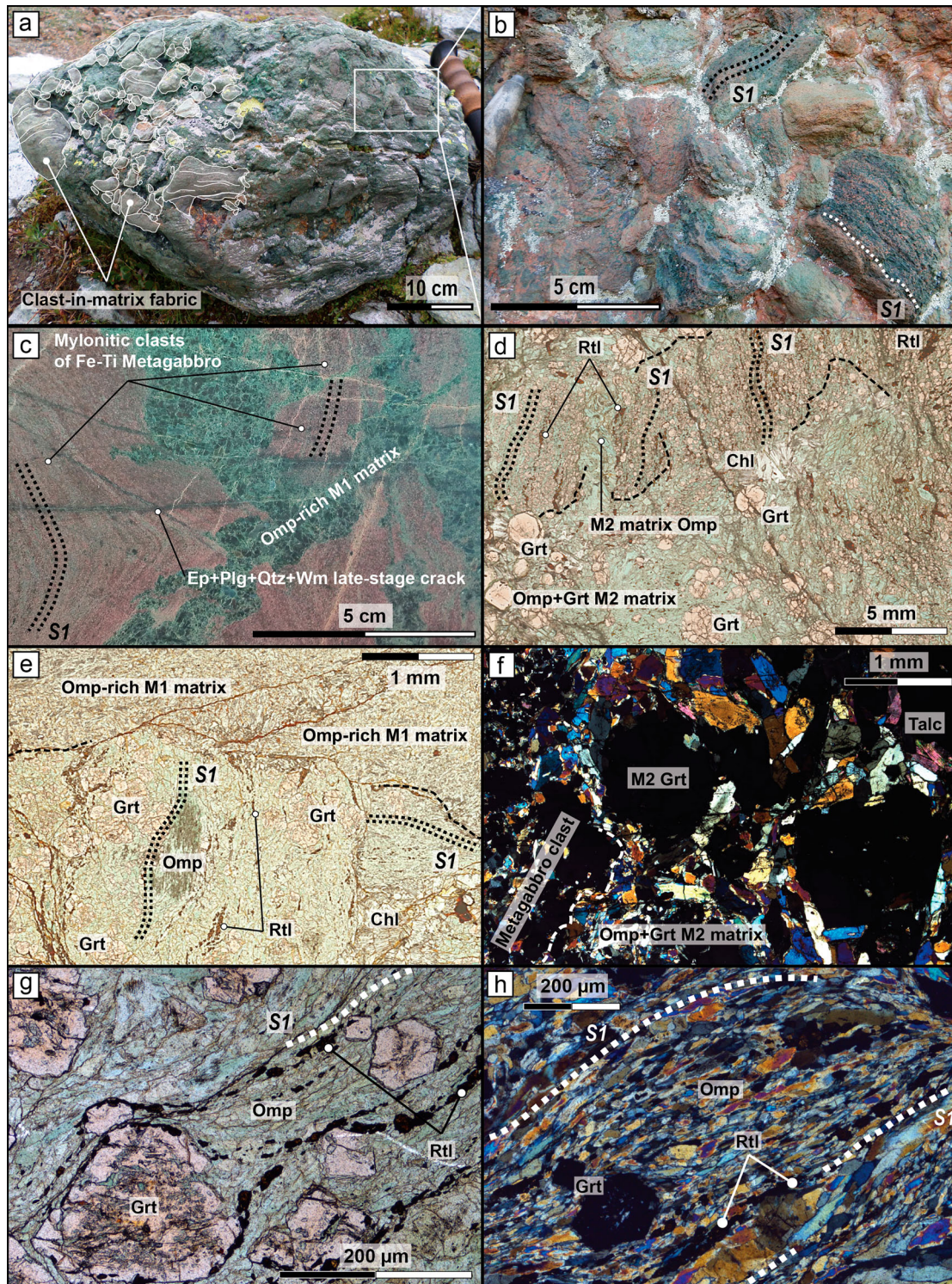


**Figure 6.** (a) Type1, eclogite-breccia block. The clast-in-matrix structure with foliated and rotated clasts is well preserved under the pervasive lichen cover. Block from the upper Bulé Valley, NE of Colle di Luca pass. (b) Typical fabric of eclogite-breccia blocks and layers at the cm-scale: the clast-in-matrix structure is emphasized by the foliated clasts of Fe-Ti metagabbro composition, with the S1 well preserved and underlined by garnet + rutile + omphacite beds. (c) Polished rock-wedge with mm-scale, unfoliated omphacite (M1 matrix) cementing clasts composed of finely-foliated and folded Fe-Ti metagabbro. Sample L17-01, from the Fe-Ti metagabbro sliver at the base of Truc Bianco peak. (d-e) Clast-in-matrix fabric at the thin-section scale (plane-polarized light): Fe-Ti metagabbro clasts are easily recognizable by the development of pervasive foliation underlined by rutile trails and the occurrence of mm-scale omphacite porphyroblasts. Differently, matrices M1 (omphacite-rich) and M2 (omphacite + garnet-rich) are unfoliated and show diffused metasomatism leading to the crystallization of newly-formed garnet, chlorite, talc and amphiboles. Thin sections LSZ63-15b from the Fe-Ti metagabbro sliver at the base of Truc Bianco and LSZ14-53 from the block B51, east of Peiro Jauno peak. (f) Cross-polarized light photomicrograph of the big hypidiomorphic omphacite crystals and the inclusion-poor garnets constituting the bulk of M2 matrix. In evidence, again, the lack of any foliation in the eclogitic matrix. Sample L63-15b, LSZ. (g-h) Mylonitic, eclogite-facies foliation of a Fe-Ti metagabbro clasts (sample L14-50, LSZ) underlined by rutile trails and flattened omphacite crystals (aspect ratio up-to 1:20). Picture 4g: plane-polarized light; Picture 4h: cross-polarized light.

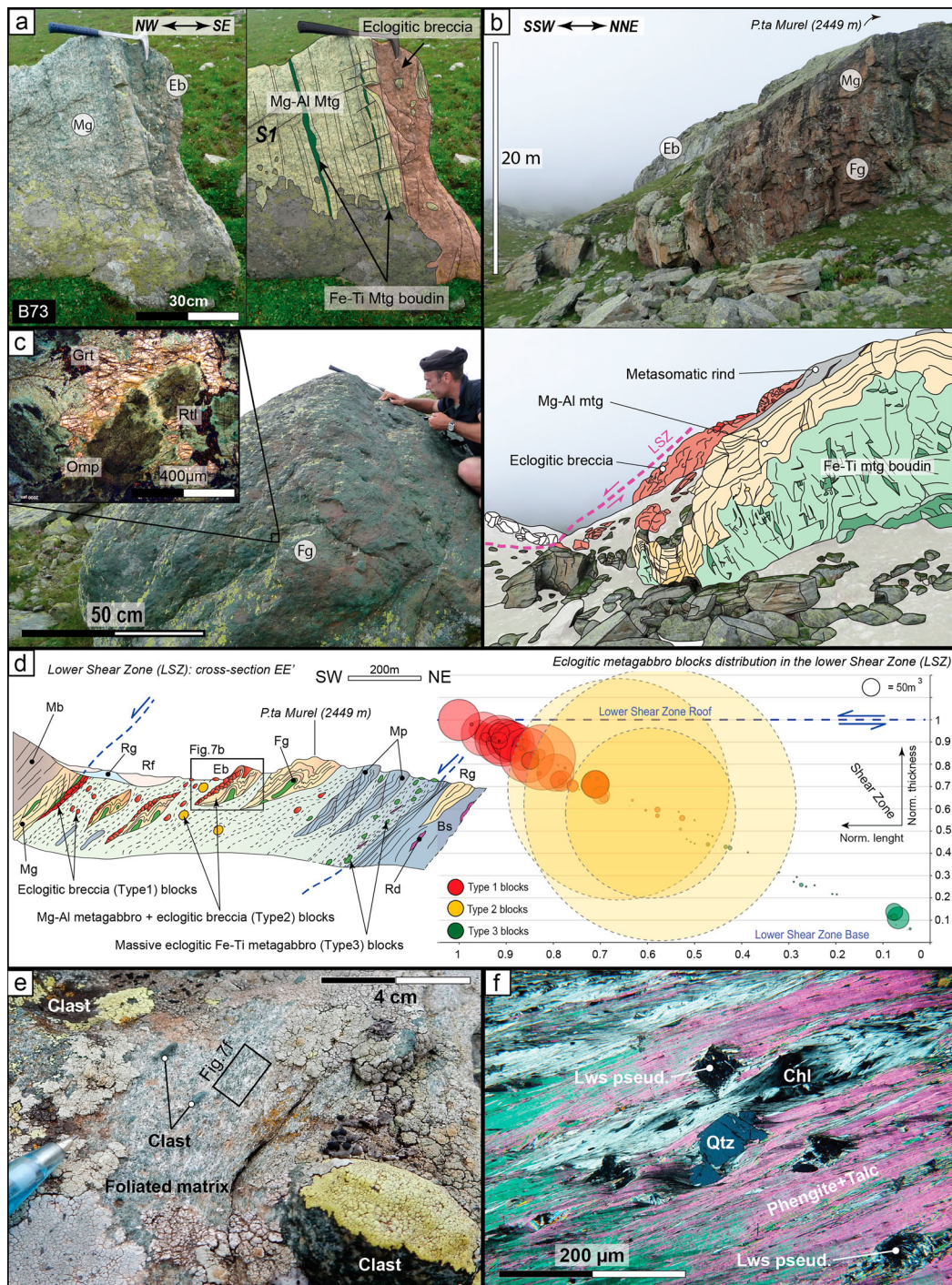


**Figure 7.** (a) Typical structures developed inside a **Type2** block, with the breccia layer crosscutting (here sub-parallelly) the S1 foliation of the Mg-Al metagabbro. Block B63, Pra Fiorito valley. (b) A dam-scale sliver of mylonitic, complexly-folded Mg-Al metagabbro (Mg) enclosing m-scale boudins of Fe-Ti metagabbros (Fg) both cut by eclogite-facies breccia (Eb) layers dipping toward the hangingwall of the LSZ (west). To be noted the structural analogies with the smaller Type2 blocks. Punta Murel, LSZ. (Field photograph at the top and its redrawn sketch at the bottom). (c) Massive block of Fe-Ti metagabbro at the base of the LSZ. This type of blocks (Type3) are characterized by the lack of any breccia structure. In the box: microphotograph of a domain composed of low-strained Fe-Ti metagabbro, characterized by the topotactic crystalization of coronitic garnet around omphacite megacrysts. More details in the text. Block B12, SW of Rocca Nera. (d) Geological section across the Lower Shear Zone (Punta Murel area) and diagram showing the distribution of metagabbro blocks inside the LSZ. Note how eclogite breccia layers are distributed in an orderly manner (dip towards West) in the detached Mg-Al metagabbros slices dispersed in the LSZ. Unbrecciated Fe-Ti metagabbro blocks (Type3) are concentrated at the base of LSZ, whereas most of the eclogite breccia blocks (Type 1) outcrop in the upper part, above the Mg-Al metagabbro slices. In the diagram the X-axis represents the normalized horizontal distance of blocks from the base of LSZ and on Y-axis the normalized vertical distance of blocks from the base of LSZ. The distribution was analyzed only for the blocks still enveloped in the syn-S2 matrix of the LSZ. (e) Close-up view of a foliated matrix cementing a polymictic conglomerate in a metasedimentary sliver from the LSZ (Prà Fiorito Valley). In evidence the rounded clasts, that locally appear to be strongly flattened parallelly to the foliation planes. (f) Photomicrograph of the sedimentary-derived matrix of Figure 5(e) (cross-polarized light). Here, differently from eclogite-facies breccias, the matrix is mainly composed of phengite + talc ± omphacite with subordinate chlorite, ex-lawsonite, garnet and quartz porphyroblasts enveloped in the strongly developed foliation.

Most Type2 (76%) and all Type1 blocks are located stratigraphically above the big slivers of retrogressed Mg-Al metagabbro of Punta Murel, Colle di Luca and Alpetto Lake (Type2). Unbrecciated Type3 blocks, which are restricted to a 30–100 m thick-band at the base of the LSZ, show a general volume increase towards the serpentinite sole (Figure 7(d)).

### 6.1.2. Other blocks in the LSZ

Blocks of other lithologies in the LSZ include metaperidotites (almost completely serpentinitized), rodingitic-metagabbro dykes and rare m-size blocks of jadeitite (see: Locatelli et al., 2018 for details).

M-scale lenses of eclogite-facies metasediments are also dispersed within the LSZ, lacking a well-defined stratigraphical position and decreasing in abundance from N to S. Large slivers (up to 90 m thick) were only observed in Lago Superiore, Pra Fiorito and Alpetto area. These preserve evidence for alternations of metadolostones, quartz-mica-rich metasandstones, micaschists, calcschists, metacherts and meta-conglomerate strata. The latter, frequently clast-supported, are composed of mm- to dm-sized (<50 cm) clasts made of gabbro, basalt and peridotite mixed inside a strongly deformed sedimentary matrix (Figure 7(e) and (f)). Clasts are well rounded and elongated (aspect ratio up to 4), often boudinated and indicative of strong deformation.

## 7. Discussion

Metagabbro breccia blocks equilibrated at eclogite-facies P-T conditions (i.e. omphacite + garnet + rutile paragenesis in both clast and matrices; Figure 6(c–f)) resulting from brittle rupture at 80 km depth (Angiboust, Langdon, et al., 2012; Locatelli et al., 2018).

The main eclogite-facies brecciation structures in metagabbros (further petrographic and microstructural details in Locatelli et al., 2018) are the following:

- (i) all the breccia planes preserved in eclogitic blocks cut abruptly, at various angles, the mylonitic eclogite facies foliation inside intact Mg-Al metagabbros with Fe-Ti metagabbro boudins (e.g. Type 2 blocks; Figure 7(a)).
- (ii) eclogitic breccias are almost monogenic (clasts: ~90% of Fe-Ti metagabbros; e.g. Figure 6(b–e)), with minor Mg-Al metagabbro clasts (~10%) restricted to the rims (20–50 cm zones) of breccia planes crosscutting Mg-Al metagabbros.
- (iii) within the breccia planes, Fe-Ti and Mg-Al clasts show evidence for ductile deformation at eclogite-facies conditions (e.g. grain boundaries migration in omphacite, growth of syn-kinematic garnet crystals; Figure 6(d–h)) with misorientation of their internal mylonitic foliation.

- (iv) crystallization of matrices with typical eclogite facies paragenesis (omphacite ± garnet ± lawsonite; Figure 6(c–f)) testifies that brecciation occurred at eclogite facies conditions.
- (v) Inside metabreccia blocks, the lack of any foliation in the eclogitic matrices enveloping plastically-deformed clasts (e.g. preserving S1; Figure 6(b–h)) demonstrates pristine brecciation at eclogite-facies condition. For the same reason, processes of static overprint of pre-subduction structures (e.g. foliated sedimentary conglomerates and/or detachment fault breccias) must be excluded.

Moreover, field mapping shows that the ~90% of Type 2 blocks and all Type 1 blocks (both types bearing eclogitic breccia) crop out in the upper part of the LSZ, structurally above the large slivers of Mg-Al metagabbros found all along the strike of the shear zone from Colle di Luca to Ghincia Pastour (Figure 7(d)). Therefore, eclogite-facies brecciation preferentially occurred on Fe-Ti metagabbros either located (i) structurally above the Mg-Al metagabbros (directly below the metabasalts along the ISZ) or (ii) along dykes and/or sills of Fe-Ti metagabbros emplaced within the Mg-Al metagabbro sequence (e.g. east of Truc Bianco cliff).

Mg-Al and Fe-Ti metagabbro intrusions (the latter locally rodingitized) are also found in the basal peridotite (Figure 3(c)), likewise in active slow-spreading oceans such as the Indian Ocean and the Mid-Atlantic ridge (i.e. Dick, Tivey, & Tucholke, 2008; Lagabrielle & Cannat, 1990; Lagabrielle & Lemoine, 1997; Lissenberg, Rioux, Shimizu, Bowring, & Mével, 2009). Such unbrecciated, coarse grained Fe-Ti metagabbro (Type3 blocks, with size decreasing towards the basal peridotite; Figure 7(c)) are restricted to the lower part of the LSZ (Figure 7(d)) and may correspond to sills or dykes intruded into the peridotite sole (e.g. Dick et al., 2008), progressively incorporated into the LSZ during shear zone widening (Locatelli et al., 2018).

Thus, the observation that (i) in Mg-Al metagabbro Type2 blocks the eclogitic breccia planes always broadly dip to SW (e.g. on their upper/western side: Punta Murel and Colle di Luca; Figure 7(b)) and (ii) breccia blocks are systematically distributed in the upper part of the LSZ (Figure 7(d)) report limited mixing and rotation after their dissemination in the shear zone. Furthermore, the ordered decreasing of block size inside the LSZ (Figure 7(d)) attests for development of the shear zone by network widening, with progressive migration of strain localization from the top to the base (further details in Locatelli et al., 2018). Finally, the occurrence of only rare type 1 blocks dispersed in the ISZ without any type 2 and 3 blocks suggests that discrete eclogitic brecciation occurred in both LSZ and ISZ, rather than a unique brittle event in the ISZ with subsequent fragments disruption and

further incorporation into the LSZ (as envisioned by Angiboust, Langdon, et al., 2012). This latter would imply km-scale movements, ramp faults between the ISZ and LSZ and greater disruption and/or mixing of blocks, whose evidence are not found in the Monviso metaophiolite.

Distinct blocks nevertheless preserve evidence for pre-eclogitic disruption (e.g. Locatelli et al., 2018). Conglomeratic layers, containing well rounded clasts of metagabbro, metabasalt and serpentinite, were found in both the LSZ and USZ (e.g. Figure 7(e) and (f)). In contrast to the above eclogitic breccia, however, clasts are embedded in strongly deformed, mylonitic matrices with continuous foliation (even if folded) cutting-across matrix and clasts. These structures, advocating for the coeval eclogitic mylonitization of former clasts and surrounding matrix, could correspond to pre-alpine sedimentary or tectonic breccias, ascribed to detachment faulting (Balestro et al., 2015; Festa et al., 2015).

## 8. Conclusions

This map provides new insights into a long-studied area of the Western Alps, the Monviso Massif. It supplies an unprecedented detail on the distribution of eclogite-facies metagabbro blocks inside the LSZ and ISZ crosscutting the LSU.

These blocks contain, among other lithologies, breccias composed of eclogite-facies matrices cementing mylonitic clasts. The latter consist of eclogite-facies metagabbros developing syn-eclogitic foliation whereas the matrices shows static crystallization and therefore the breccias are interpreted as the result of brecciation at high-pressure conditions.

Their predominance inside the LSZ, with ordered distribution in the shear zone matrix, with top-to-base blocks size reduction and limited evidence for (i) mixing and (ii) rotation, advocate for the development of the LSZ at HP-condition rather than reactivation of pre-alpine structures. Inside the LSZ, the evidence for protracted mixing only at the footwall, advocates for shear zone development by network widening, with progressive migration of strain localization from the top to the base.

Finally, the presence of only rare eclogitic breccia blocks inside the ISZ (without any Type2 and Type3 blocks, found in the LSZ only) suggests that eclogite-facies brecciation occurred as distinct events, active in both the shear zones.

## Software

The map has been drawn using the software ESRI Arc-Gis10<sup>®</sup> and Adobe illustrator CS6. GPS data were acquired with a Garmin Dakota<sup>®</sup> device and processed with dedicated BaseCamp<sup>™</sup> software. Aerial and

satellite images were analysed on google Earth Pro<sup>™</sup> software.

The structural data were analysed with the software OpenStereo<sup>®</sup>. Photographs were processed through Fiji<sup>®</sup> image-analysis (Schindelin et al., 2012) and Paint softwares.

## Acknowledgements

This study was funded by the project ‘Zooming in between plates’ (Marie Curie International Training Network no. 604713). We thank E. Delairis (ISTeP) for the preparation of thin sections and the Parco del Monviso for the bureaucratic support. We also thank the friends of Rifugio Alpetto for the gastronomic and moral support. Silvana Martin, Giovanni Capponi, Andrej Spiridonov, Heike Apps and Arthur Merschat are warmly thanked for their constructive reviews and suggestions, and Mike J. Smith for his editorial handling leading to a significant improvement of the manuscript.

## Disclosure statement

No potential conflict of interest was reported by the authors.

## Funding

This study was funded by the project ‘Zooming in between plates’ (Marie Curie International Training Network no. 604713).

## ORCID

Michele Locatelli  <http://orcid.org/0000-0002-8753-1693>

## References

- Agard, P., Monié, P., Jolivet, L., & Goffé, B. (2002). Exhumation of the Schistes Lustres complex: In situ laser probe <sup>40</sup>Ar/<sup>39</sup>Ar constraints and implications for the Western Alps. *Journal of Metamorphic Geology*, 20, 599–618.
- Agard, P., Yamato, P., Jolivet, L., & Burov, E. (2009). Exhumation of oceanic blueschists and eclogites in subduction zones: Timing and mechanisms. *Earth-Science Reviews*, 92, 53–79. <https://doi.org/10.1016/j.earscirev.2008.11.002>
- Angiboust, S., Agard, P., Raimbourg, H., Yamato, P., & Huet, B. (2011). Subduction interface processes recorded by eclogite-facies shear zones (Monviso, W. Alps). *Lithos*, 127, 222–238. <https://doi.org/10.1016/j.lithos.2011.09.004>
- Angiboust, S., Agard, P., Yamato, P., & Raimbourg, H. (2012). Eclogite breccias in a subducted ophiolite: A record of intermediate-depth earthquakes? *Geology*, 40, 707–710. <https://doi.org/10.1130/G32925.1>
- Angiboust, S., Langdon, R., Agard, P., Waters, D., & Chopin, C. (2012). Eclogitization of the Monviso ophiolite (W. Alps) and implications on subduction dynamics. *Journal of Metamorphic Geology*, 30, 37–61. <https://doi.org/10.1111/j.1525-1314.2011.00951.x>
- Angiboust, S., Pettke, T., De Hoog, J. C. M., Caron, B., & Oncken, O. (2014). Channelized fluid flow and eclogite-facies metasomatism along the subduction shear zone.

- Journal of Petrology*, 55, 883–916. <https://doi.org/10.1093/petrology/egu010>
- Balestro, G., Festa, A., Borghi, A., Castelli, D., Gattiglio, M., & Tartarotti, P. (2018). Role of late Jurassic intra-oceanic structural inheritance in the Alpine tectonic evolution of the Monviso meta-ophiolite complex (Western Alps). *Geological Magazine*, 155, 233–249. <https://doi.org/10.1017/S0016756817000553>
- Balestro, G., Festa, A., & Tartarotti, P. (2015). Tectonic significance of different block-in-matrix structures in exhumed convergent plate margins: Examples from oceanic and continental HP rocks in inner Western Alps (northwest Italy). *International Geology Review*, 57, 581–605. <https://doi.org/10.1080/00206814.2014.943307>
- Balestro, G., Fioraso, G., & Lombardo, B. (2013). Geological map of the Monviso massif (Western Alps). *Journal of Maps*, 9, 623–634. <https://doi.org/10.1080/17445647.2013.842507>
- Balestro, G., Lombardo, B., Vaggelli, G., Borghi, A., Festa, A., & Gattiglio, M. (2014). Tectonostratigraphy of the northern Monviso meta-ophiolite complex (Western Alps). *Italian Journal of Geosciences*, 133, 409–426.
- Blake, M. C. Jr, Moore, D. E., & Jayko, A. S. (1995). *The role of serpentinite melanges in the unroofing of UHPM rocks: An example from the Western Alps of Italy*. Metamorph: Ultrah Press. 182–205.
- Castelli, D., Rostagno, C., & Lombardo, B. (2002). Jd-qtz-bearing metaplagiogrinite from the monviso meta-ophiolite (western Alps). *Ofoliti*, 27, 81–90. <https://doi.org/10.4454/ofoliti.v27i2.178>
- Cliff, R. A., Barnicoat, A. C., & Inger, S. (1998). Early Tertiary eclogite facies metamorphism in the Monviso Ophiolite. *Journal of Metamorphic Geology*, 16, 447–455. <https://doi.org/10.1111/j.1525-1314.1998.00147.x>
- Compagnoni, R., Rolfo, F., Manavella, F., & Salusso, F. (2007). Jadeitite in the Monviso meta-ophiolite, Piemonte zone, Italian Western Alps. *Periodico di Mineralogia*, 76, 79–89.
- Coward, M., & Dietrich, D. (1989). Alpine tectonics – An overview. *Geological Society, London, Special Publications*, 45, 1–29. <https://doi.org/10.1144/GSL.SP.1989.045.01.01>
- De La Pierre, F., Lozar, F., & Polino, R. (1997). L'utilizzo della tettonostratigrafia per la rappresentazione cartografica delle successioni metasedimentarie nelle aree di catena. *Mémoires de la Société Géologique de France Paléontologie*, 49, 195–206.
- Dick, H. J. B., Tivey, M. A., & Tucholke, B. E. (2008). PLutonic foundation of a slow-spreading ridge segment: Oceanic core complex at Kane Megamullion, 23° 30' N, 45° 20' W. *Geochem Geophys Geosystems* 9. <https://doi.org/10.1029/2007GC001645>
- Dutto, F., Godone, F., & Mortara, G. (1991). L'écroulement du glacier supérieur de Coolidge. (Paroi nord du Mont Viso, Alpes occidentales). *Revue de Géographie Alpine*, 79, 7–18. <https://doi.org/10.3406/rga.1991.3597>
- Festa, A., Balestro, G., Dilek, Y., & Tartarotti, P. (2015). A Jurassic oceanic core complex in the high-pressure Monviso ophiolite (western Alps, NW Italy). *Lithosphere*, 7, 646–652. <https://doi.org/10.1130/L458.1>
- Festa, A., Pini, G. A., Dilek, Y., & Codegone, G. (2010). Mélanges and mélange-forming processes: A historical overview and new concepts. *International Geology Review*, 52, 1040–1105. <https://doi.org/10.1080/00206810903557704>
- Gastaldi, B. (1876). Spaccato geologico lungo le valli superiori del Po e delle Varaita. *B.C.G.I.*, 7, 104–111.
- Groppo, C., & Castelli, D. (2010). Prograde P-T evolution of a lawsonite eclogite from the monviso meta-ophiolite (Western Alps): Dehydration and redox reactions during subduction of oceanic FeTi-oxide gabbro. *Journal of Petrology*, 51, 2489–2514. <https://doi.org/10.1093/petrology/egq065>
- Guillot, S., Schwartz, S., Hattori, K., Auzende, A., & Lardeaux, J. (2004). The Monviso ophiolitic massif (Western Alps), a section through a serpentinite subduction channel. *Journal of the Virtual Explorer*, 16, 17.
- Lagabrielle, Y., & Cannat, M. (1990). Alpine Jurassic ophiolites resemble the modern central Atlantic basement. *Geology*, 18, 319–322. [https://doi.org/10.1130/0091-7613\(1990\)018<0319:AJORTM>2.3.CO;2](https://doi.org/10.1130/0091-7613(1990)018<0319:AJORTM>2.3.CO;2)
- Lagabrielle, Y., & Lemoine, M. (1997). Alpine, Corsican and Apennine Ophiolites: The slow-spreading ridge model. *Comptes Rendus de l'Académie des Sciences – Series IIA – Earth and Planetary Science*, 325, 909–920. [https://doi.org/10.1016/S1251-8050\(97\)82369-5](https://doi.org/10.1016/S1251-8050(97)82369-5)
- Laubscher, H. (1991). The arc of the Western Alps today. *Eclogae Geologicae Helvetiae*, 84, 359–631.
- Lissenberg, C. J., Rioux, M., Shimizu, N., Bowring, S. A., & Mével, C. (2009). Zircon dating of oceanic crustal accretion. *Science*, 323, 1048–1050. <https://doi.org/10.1126/science.1167330>
- Locatelli, M., Verlaquet, A., Agard, P., Federico, L., & Angiboust, S. (2018). Intermediate-depth brecciation along the subduction plate interface (Monviso eclogite, W. Alps). *Lithos*, 320–321, 378–402. <https://doi.org/10.1016/j.lithos.2018.09.028>
- Lombardo, B. (1978). Osservazioni preliminari sulle ofioliti metamorfiche del Monviso (Alpi Occidentali). *Rendiconti Della Società Italiana di Mineralogia e Petrologia*, 34, 235–305.
- Lombardo, B., Rubatto, D., & Castelli, D. (2002). Ion microprobe U-PB dating of zircon from a Monviso metaplagiogrinite: Implications for the evolution of the Piedmont-Liguria tethys in the Western Alps. *Ofoliti*, 27, 109–117.
- Malusà, M.G., Faccenna, C., Garzanti, E., Polino, R. (2011). Divergence in subduction zones and exhumation of high pressure rocks (Eocene Western Alps). *Earth Planetary Science Letters*, 310, 21–32. <https://doi.org/10.1016/j.epsl.2011.08.002>
- Marthaler, M., & Stampfli, G. M. (1989). Les Schistes lustrés à ophiolites de la nappe du Tsaté: un ancien prisme d'accrétion issu de la marge active apulienne? *Schweizerische Mineralogische und Petrographische Mitteilungen*, 69, 211–216.
- Messiga, B., Kienast, J. R., Rebay, G., Riccardi, M. P., & Tribuzio, R. 1999. Cr-rich magnesiochloritoid eclogites from the Monviso ophiolites (Western Alps, Italy). *Journal of Metamorphic Geology*, 17, 287–299. <https://doi.org/10.1046/j.1525-1314.1999.00198.x>
- Mortara, G. & Dutto, F. (1990). Un episodio parossistico nell'evoluzione dei ghiacciai del gruppo del Monviso: il crollo del Ghiacciaio Superiore di Coolidge. *Geografia Fisica e Dinamica Quaternaria*, 13, 187–189.
- Nadeau, S., Philippot, P., & Pineau, F. (1993). Fluid inclusion and mineral isotopic compositions (H-C-O) in eclogitic rocks as tracers of local fluid migration during high-pressure metamorphism. *Earth and Planetary Science Letters*, 114, 431–448.
- Novarese, V. (1895). Nomenclatura e sistematica delle rocce verdi nelle Alpi Occidentali. *B.C.G.I.*, 26, 164–181.
- Philippot, P. (1987). “Crack seal” vein geometry in eclogitic rocks. *Geodinamica Acta*, 1, 171–181. <https://doi.org/10.1080/09853111.1987.11105136>

- Philippot, P., & Kienast, J.-R. (1989). Chemical-microstructural changes in eclogite-facies shear zones (Monviso, Western Alps, north Italy) as indicators of strain history and the mechanism and scale of mass transfer. *Lithos*, 23, 179–200. [https://doi.org/10.1016/0024-4937\(89\)90004-2](https://doi.org/10.1016/0024-4937(89)90004-2)
- Philippot, P., & Selverstone, J. (1991). Trace-element-rich brines in eclogitic veins: Implications for fluid composition and transport during subduction. *Contributions to Mineralogy and Petrology*, 106, 417–430. <https://doi.org/10.1007/BF00321985>
- Philippot, P., & van Roermund, H. L. M. (1992). Deformation processes in eclogitic rocks: Evidence for the rheological delamination of the oceanic crust in deeper levels of subduction zones. *Journal of Structural Geology Mechanical Instabilities in Rocks and Tectonics*, 14, 1059–1077. [https://doi.org/10.1016/0191-8141\(92\)90036-V](https://doi.org/10.1016/0191-8141(92)90036-V)
- Plunder, A., Agard, P., Chopin, C., & Okay, A. I. (2013). Geodynamics of the Tavşanlı zone, western Turkey: Insights into subduction/obduction processes. *Tectonophysics*, 608, 884–903. <https://doi.org/10.1016/j.tecto.2013.07.028>
- Pognante, U., & Kienast, J.-R. (1987). Blueschist and eclogite transformations in Fe-Ti gabbros: A Case from the Western Alps Ophiolites. *Journal of Petrology*, 28, 271–292. <https://doi.org/10.1093/petrology/28.2.271>
- Ricou, L. E., & Siddans, A. W. B. (1986). Collision tectonics in the Western Alps. *Geological Society, London, Special Publications*, 19, 229–244. <https://doi.org/10.1144/GSL.SP.1986.019.01.13>
- Rubatto, D., & Angiboust, S. (2015). Oxygen isotope record of oceanic and high-pressure metasomatism: A P–T–time–fluid path for the Monviso eclogites (Italy). *Contributions to Mineralogy and Petrology*, 170, 1–16. <https://doi.org/10.1007/s00410-015-1198-4>
- Rubatto, D., & Hermann, J. (2003). Zircon formation during fluid circulation in eclogites (Monviso, Western Alps): implications for Zr and Hf budget in subduction zones. *Geochimica et Cosmochimica Acta*, 67, 2173–2187. [https://doi.org/10.1016/S0016-7037\(02\)01321-2](https://doi.org/10.1016/S0016-7037(02)01321-2)
- Schindelin, J., Arganda-Carreras, I., Frise, E., Kaynig, V., Longair, M., Pietzsch, T., ... Cardona, A. (2012). Fiji: An open-source platform for biological-image analysis. *Nature Methods*, 9, 676–682. <https://doi.org/10.1038/nmeth.2019>
- Schmid, S. M., & Kissling, E. (2000). The arc of the western Alps in the light of geophysical data on deep crustal structure. *Tectonics*, 19, 62–85. <https://doi.org/10.1029/1999TC900057>
- Schwartz, S., Lardeaux, J.-M., Guillot, S., & Tricart, P. (2000). Diversité du métamorphisme écolitique dans le massif ophiolitique du Monviso (Alpes occidentales, Italie). *Geodinamica Acta*, 13, 169–188. <https://doi.org/10.1080/09853111.2000.11105371>
- Spandler, C., Pettke, T., & Rubatto, D. (2011). Internal and External Fluid Sources for eclogite-facies veins in the Monviso meta-ophiolite, Western Alps: Implications for Fluid Flow in subduction zones. *Journal of Petrology*, 52, 1207–1236. <https://doi.org/10.1093/petrology/egr025>
- Stella, A. (1895). Sul rilevamento geologico eseguito nel 1894 in valle Varaita (Alpi Cozie). *B.C.G.I.*, 26, 283–313.
- Zaccagna, D. (1887). Sulla geologia delle Alpi Occidentali. *B.C.G.I.*, 18, 346–417.

## Appendix

Complete list of the acronym used in the text and in the map. Units: MU, Monviso Unit; LSU, Lago Superiore Unit. Sub-units: LSS, Lago Superiore Sub-unit; LSZ, Lower Shear Zone Sub-unit; BSS, Basal Serpentinite Sub-unit. Other shear zones: USZ, Upper Shear Zone; ISZ, Intermediate Shear Zone. Lithologies: Mus, metasediments of Monviso Unit; Fb, metabasites of Monviso Unit; Eb, eclogite-facies metabasites; Ms, metasediments of Lago Superiore Sub-unit; Mb, metabasites of Lago Superiore Sub-unit; Fg, Fe-Ti metagabbros; Mg, Mg-Al metagabbros; Rg, retrogressed Mg-Al metagabbros; Mt, metatroctolites; Mp, massive metaperidotites; Rd, rodingitic dykes; Ss, strongly deformed mylonitic serpentinite schists; Bs, foliated to massive antigorite-rich serpentinites. Quaternary: Df, Alluvial and debris deposits; Td, recent talus deposits; Ag and Ug, undifferentiated glacial deposits; Ir, inactive rock glacier; Sf, glaciers and perennial snow patches. Further details in the 1:20.000 map legend.